https://doi.org/10.1016/j.nanoen.2016.11.050 This is the Pre-Published Version.

Hydroelectric generator from transparent flexible zinc oxide nanofilms

Xuemei Li,[1] Chun Shen,[1] Qin Wang,[1] Chi Man Luk,[2] Baowen Li,[1] Jun Yin,[1] Shu Ping Lau,[2] Wanlin Guo[1†]

1. State Key Laboratory of Mechanics and Control of Mechanical Structures, the Key Laboratory of Intelligent Nano Materials and Devices of DoE, Institute of Nano Science of Nanjing University of Aeronautics and Astronautics, Nanjing 210016, China

2 . Department of Applied Physics, the Hong Kong Polytechnic University, Hung Hom, Kowloon, Hong Kong S.A.R., P.R. China

† E-mail: wlguo@nuaa.edu.cn

Harvesting wave energy based on waving potential, a newly found electrokinetic effect, is attractive but limited mainly to monolayer graphene. Here we demonstrate that moving a transparent flexible ZnO nanofilm across the surface of ionic solutions can generate electricity. The generated electricity increases linearly with the moving velocity with an open-circuit voltage up to tens of millivolt and a short-circuit current at the order of microampere. The harvested electricity can be efficiently scaled up through series and parallel connections. Theoretical simulations show that it is the proper electrical property that endows the ZnO nanofilm with the outstanding capacity in harvesting the wave energy.

Keywords: Zinc oxide nanofilm, Energy harvest, Wave energy, Transparent, Flexible, Waving potential

© 2016. This manuscript version is made available under the CC-BY-NC-ND 4.0 license https://creativecommons.org/licenses/by-nc-nd/4.0/.

Introduction

In the pursuit of high-efficient energy conversion technology, nanomaterials offer much promise due to their exceptional sensitivity to external stimulations.[1-5] The great achievements in nanogenerators based on piezoelectric and triboelectric effect have stimulated tremendous passions in the exploration of environmental energy harvesting by nanomaterials.[1, 6-10] Ceaseless waving seawater covers more than 70% of the surface of the earth, thus possessing inexhaustible energy.[11] Capturing the wave energy could have special importance for powering intelligent devices in remote ocean. However, the effective strategy is underexplored,[12-13] and traditional approaches based on electromagnetic effect face socioeconomic challenges and also bring up biophysical impacts on the marine environment.[14] Use of nanomaterials to harvest wave energy is an emerging trend with promising prospect in terms of cost and efficiency.[15-18]

Recently, we found that a monolayer graphene sheet placed across the surface of waving water can generate electricity, which is referred to as waving potential, providing a novel electrokinetic pathway to harvest wave energy.[19-20] The waving potential is created by moving boundary of the electrical double layer (EDL) formed at the interface of graphene and ionic solutions. However, the waving potential drops sharply when the layer number of graphene increases to two and three, and almost vanishes for other materials including graphite, gold, copper and silicon with thickness over tens of nanometers[19], hindering the applications of waving potential. Therefore, cost-efficient, transparent and flexible substitutions of graphene is highly desired.[19-20]

Zinc oxide (ZnO) is a wide band gap (~3.37 eV) semiconducting material with outstanding electrical and optical properties.[21] The hexagonal wurtzite structure endows ZnO with a notable piezoelectric property, giving rise to enormous applications, especially in piezoelectric nanogenerators.[1, 6, 22] ZnO nanofilms can now be prepared facilely by sol-gel techniques, pulsed laser deposition and filtered cathodic vacuum arc in large area at low cost.[23-27] These processes can be conducted at room temperature and, [27] thus, ZnO can be deposited directly onto plastic and

flexible substrates. Moreover, ZnO nanofilms show good transparence over the entire visible spectrum. Given these advantages, ZnO nanofilms would be a promising candidate if showing notable waving potential effect.[28-29]

Here we demonstrate that the ZnO nanofilm prepared through filtered cathodic vacuum arc can generate voltage up to tens of millivolts when moving across the interface of ionic solution and air. The influences of interval time between two moving cycles, velocity, ions concentration, have been comprehensively investigated, showing the versatility of ZnO nanofilms in harvesting ambient energy.

Experimental Section

Device fabrication and measurements. The ZnO nanofilm used in this work was sputtering deposited by filtered cathodic vacuum arc at room temperature.[27] Polyester terephthalate (PET) was selected as the substrates for its high transparency and flexibility. The PET substrates are cut into 4×8 cm^2 size and the thickness of ZnO film was controlled to be around 50 nm by adjusting the deposition time. The oxygen pressure was kept at 1×10^{-4} Torr during the deposition to maintain a square resistance of the obtained ZnO film around 20 kohm. Large area scanning electron microscopy (SEM) image (Fig. 1a) indicates a smooth and uniform surface of the sample. The high-magnification atomic force microscopy (AFM) topography image (Fig. 1b) shows that the film comprises grains of typical size around 10 nm. X-ray diffraction spectrum (Fig. S1) shows a significantly broadening peak corresponding to (201) direction, indicating a ultra-small grain size and the presence of nonuniform stress distribution. Two terminals along the length of ZnO nanofilm were connected to copper wires by silver emulsion with robust ohmic contact for the electric measurement. To avoid the direct exposure of metal electrodes to the ionic solution,[30] the electrodes were completely sealed with silicone. The voltage signal across the ZnO samples was recorded by a Keithley 2010 multimeter, and the current was measured by a Keithley 2400 multimeter. These meters were implemented by a controlling software with a sampling rate around 20 s^{-1}.

COMSOL simulations. We compared the electrostatic potential distribution in ZnO and metallic nanofilms during the formation of EDL on newly wetted surface using the COMSOL package. The ZnO and metallic nanofilms were simulated as plates of infinite width. The length and the thickness of the plates are 1 μm and 50 nm, respectively. The carrier concentrations of the nanofilms are set to be 1×10^{20} cm^{-3} for ZnO [27] and 1×10^{22} cm^{-3} for metallic nanofilm. The corresponding mobilities are 1 cm^2 V^{-1} s^{-1} [27] and 390 cm^2 V^{-1} s^{-1}, respectively. To simulate the process of cation adsorption on newly wetted surface, the concentration of the Na^+ layer for the left 2/5 section of the plates increases from 0 to 0.01 mol/L step-by-step with a step of 0.001 mol/L, while both the Na^+ layer and Cl^- layer are set to be of a concentration of 0.01 mol/L with a thickness of 1 nm for the remainder 3/5 section of the plane. Based on the specific adsorption for each step, corresponding electrostatic potential distribution was calculated respectively.

Results and discussions

Figures 1a and 1b show the photographs of a ZnO nanofilm sample, highlighting its transparence and flexibility. Figure 1c shows a schematic illustration of the experimental setup. The ZnO sample was inserted into and then pulled out from 0.6 M NaCl solution (～ 3.5 wt% as seawater) periodically at a constant velocity, which is controlled by a variable-speed motor (Fig. S2). The typical electric voltage signal recorded during one inserting-pulling cycle at a velocity of 13.5 cm/s was shown in Fig. 1d. There are a positive voltage peak of 7.36 mV and a negative voltage peak of -1.62 mV corresponding to the inserting and pulling process, respectively. The polarity of induced voltage suggests that the ZnO film surface prefers to adsorb Na^+ ions in NaCl solution according to the model of waving potential.[19] Once the ZnO nanofilm was inserted into the solution, a EDL consists of absorbed Na^+ layer and Cl^- ions will form at the solid-liquid interface. The accumulation of Cl^- can screen the Na^+ layer adsorbed on the ZnO surface. However, due to retarded migration of the Cl^- ions, the adsorbed Na^+ layer on ZnO section just immersed in the solution will raises the local potential. Similarly, when pulling out the ZnO sheet, the process is reversed and

the local potential of ZnO near the solution surface is reduced. The suggested mechanism is also confirmed by our dynamic simulation discussed later. The flexibility of ZnO nanofilm makes it can be fitted onto curved surface, such as a balloon buoy, and harvest the wave energy (Fig. S3).

Once completely immersing the sample into solution, we found a gradual decay of the voltage. The decay of voltage with time after the fully wetting can be well described by an exponential decay function, as shown in the insert of Fig. 1d. This exponential decay behavior is consistent with the behavior of a resistance-capacitor (RC) circuit, confirming the aforementioned EDL model as the reasonable origination of the induced voltage. As the RC time constant is proportional to the product of resistance and capacitance, the notably longer decay time for the ZnO sample compared to that of graphene can be attributed to the higher resistivity of ZnO nanofilm, providing a wide time window for collecting the generated electricity.

During the cycling measurements, we found that the peak voltage induced during the first inserting was always significantly larger than that of the following cycles. As shown in Fig. 2a, the peak voltage induced during the first inserting is up to 43 mV, which drops to around 6 mV and keeps almost constant during the following three cycles. In the meantime, the peak voltage induced by pulling almost remains stable for all the cycles. We attribute the reduction of the induced voltage in the following cycles to the hydrophilic wettability of the ZnO film. The static water contact angle of the ZnO nanofilm is around 65^{o}, as shown in the insert of Fig. 2a. The receding and advancing water contact angles are 30^{o} and 67^{o} respectively, showing a large contact angle hysteresis. Thus, once the ZnO film is wetted, it takes a relative long time for the water to slip off the surface and the ZnO film to be completely dried. If inserting the film into solution before the complete drying of the ZnO surface, only the dried surface can contribute to the induced voltage, giving rise to a reduction of the voltage value. Also, the slow de-wetting process makes the voltage value induced during the pulling process is significantly lower than that induced during the inserting process, as shown in Fig. 1d.

We further controlled the interval time between two inserting-pulling cycles, and

determined the dependence of the peak voltage on the interval time at a constant velocity of 4.2 cm/s. As shown in Fig. 2b, the inserting induced peak voltage increases with the interval time quickly and then tends to saturate around 53 mV, when the interval time is set to be 20 min. The short-circuit current can reach up to 1.3 μA at this interval time (Fig. 2c), corresponding to an output power of 47.7 nW comparable to that of graphene generator.[19] However, due to the wetting of ZnO surface, the pulling induced peak voltage keeps constant at a limited value for all the interval time. The relationship between the inserting induced peak voltage and the interval time can be well described by an exponential function (red solid line in Fig. 2b), further implying that the water evaporation plays an important role in the recovery of the induced voltage. Although the ZnO nanofilm investigated here shows deficiency in harvesting high frequency wave energy, hydrophobizating the ZnO film through morphology modulation may be an effective way to improve the performance.[31-32]

Figure 2d shows the dependence of peak voltage on the inserting velocity. Here, the interval time keeps almost the same around 5 s for different velocities. It can be seen that the peak voltage increases linearly with the velocity with a large slope for the low velocity region ($v \leqslant 13.5$ cm/s) and a small slope for the high velocity region ($v \geqslant 13.5$ cm/s). At low velocity region, the peak voltage is dominated by the migration of charge carriers in the ZnO film in correspondence to the electrical field, which tends to reduce the electrical field and reach an equilibrium state. Thus, increasing the velocity gives a short response time of the carriers, and can significantly enlarge the induced peak voltage. However, at large velocity region, the peak voltage is determined by the potential difference between anion-adsorbed ZnO and ZnO film of adsorbed electrical double layer, which is ideally a constant. Thus, the peak voltage tends to be saturated at large velocities. This is the reason why the slope for high velocity region is much small than that for low velocity region.

The influence of the NaCl concentration on the peak voltage is also investigated. Figure 2e shows the dependence of the inserting induced peak voltage on the interval time for the same sample in 0.01 M, 0.1 M and 0.6 M NaCl solutions at the same velocity of 7.8 cm/s. For all these concentrations, the peak voltage shows exponential

dependence on the interval time, as guided by the solid lines. The peak voltage increases notably with the decrease of the solution concentration in our measurement range. This can be explained by the reduced screening effect of the Cl^- layer with the decrease of the concentration. Further decreasing the NaCl concentration reduces the induced voltage due to the reduced Na^+ concentration and finally almost vanishes for DI water (Fig. S4).

The peak voltages in deionized water (DI) as well as several different salt solutions, including, NaCl, $MgCl_2$ and Na_2SO_4 solutions of the same 0.1 M concentration, are compared. The results are presented in Fig. 2f. At a velocity of 7.8 cm/s, the voltage induced in DI is negligible, only comparable to the measurement error, indicating the essential role of ions for the generation of electricity. Regarding the salt solutions, the peak voltage is largest for $MgCl_2$ solution and lowest for NaCl solution. This is attributed to the stronger charging effect of Mg^{2+} compared to that of NaCl, as confirmed by our COMSOL simulation (Fig. S5).

Previously, the waving potential is only observed in atomically thick graphene, and vanishes in various conductive materials from graphite, metals to doped semiconductor.[19] To understand the fundamental difference between ZnO and these materials with regard to their ability of harvesting wave energy, we conducted COMSOL simulation. The main difference between the ZnO and aforementioned other materials is their electrical conductivities. Thus, during the simulation, the carrier density and mobility is set to be the typical values for our ZnO sample and metal respectively, to revealing the influence of electrical conductivity to the harvesting-energy ability. The typical electric potential distribution during the adsorption of cations on newly wetted surface is shown in Fig. 3a and 3b. The deduced potential differences between the two ends of the ZnO nanofilm are tens millivolt for ZnO, two orders higher than that for metal nanofilm. This is because that the high electrical conductivity of materials like metals causes the cation-induced potential difference across the material being rapidly balanced through the transfer of electric carriers in the materials. Consequently, it can be concluded that it is the low electrical conductivity endows ZnO nanofilm with outstanding ability of harvesting

wave energy in comparison with highly conductive nanofilm.

Finally, we demonstrat that the induced electricity can be easiliy enlarged through series and parallel connections of multiple ZnO sheets. As shown in Fig. 4, the induced peak voltage of individual sample A and B is around 2 mV. Series connection of them leads to a votlage about 5mV, even larger than the sum of the two signal. This deviation may be caused by the differnce in the electric potential of the two samples in solution, giving rise to an additional contribution to the measured voltage. Similarly, through parallel connecton, the induced peak current of sample A and B increase from 0.44 μA and 0.32 μA to 0.75μA.

Conclusions

In summary, we demonstrate for the first time that moving a transparent flexible ZnO nanofilm across the surface of ionic solutions can produce voltage up to tens of millivolt. The waving potential in the ZnO nanofilm not only inherits the attractive properties previously observed in monolayer graphene, but also shows a gradually decay behavior, giving rise to a wide time window for capturing the electricity. The exponential dependence of the induced voltage on the interval time between two cycles implies the possibility of further enhancement of the induced voltage through modifying its wettability. This study highlights the potential applications of transparent flexible ZnO nanofilms in harvesting wave energy.

Acknowledgments

This work was supported by 973 program (2013CB932604, 2012CB933403), the National NSF (51472117, 91023026, 11172124, 51375240, 51002076) of China, Jiangsu Province NSF (BK20130781, BK2011722), the Research Fund of State Key Laboratory of Mechanics and Control of Mechanical Structures (0414K01), the NUAA Fundamental Research Funds (NP2015203) and the Funding of Jiangsu Innovation Program for Graduate Education (CXZZ13_0150). SPL acknowledges the support from the PolyU grant (1-ZVGH).

Supporting Information

Supplementary data associated with this article can be found in the online version.

References

[1] Z. L. Wang, J. Song, *Science* **2006**, *312*, 242.

[2] B. Tian, X. Zheng, T. J. Kempa, Y. Fang, N. Yu, G. Yu, J. Huang, C. M. Lieber, *Nature* **2007**, *449*, 885.

[3] Y. Zhu, S. Murali, M. D. Stoller, K. Ganesh, W. Cai, P. J. Ferreira, A. Pirkle, R. M. Wallace, K. A. Cychosz, M. Thommes, *Science* **2011**, *332*, 1537.

[4] W. Ma, C. Yang, X. Gong, K. Lee, A. J. Heeger, *Adv. Funct. Mater.* **2005**, *15*, 1617.

[5] R. H. Baughman, C. Cui, A. A. Zakhidov, Z. Iqbal, J. N. Barisci, G. M. Spinks, G. G. Wallace, A. Mazzoldi, D. De Rossi, A. G. Rinzler, *Science* **1999**, *284*, 1340.

[6] X. Wang, J. Song, J. Liu, Z. L. Wang, *Science* **2007**, *316*, 102.

[7] R. Yang, Y. Qin, L. Dai, Z. L. Wang, *Nat. Nanotech.* **2009**, *4*, 34.

[8] Y. Qin, X. Wang, Z. L. Wang, *Nature* **2008**, *451*, 809.

[9] F.-R. Fan, L. Lin, G. Zhu, W. Wu, R. Zhang, Z. L. Wang, *Nano Lett.* **2012**, *12*, 3109.

[10] F.-R. Fan, Z.-Q. Tian, Z. L. Wang, *Nano Energy* **2012**, *1*, 328.

[11] R. Pelc, R. M. Fujita, *Marine Policy* **2002**, *26*, 471.

[12] F. d. O. Antonio, *Renewable and sustainable energy reviews* **2010**, *14*, 899.

[13] S. H. Salter, *Nature* **1974**, *249*, 720.

[14] G. W. Boehlert, A. B. Gill, **2010**.

[15] Y. Hu, J. Yang, Q. Jing, S. Niu, W. Wu, Z. L. Wang, *ACS Nano* **2013**, *7*, 10424.

[16] Y. Su, X. Wen, G. Zhu, J. Yang, J. Chen, P. Bai, Z. Wu, Y. Jiang, Z. L. Wang, *Nano Energy* **2014**, *9*, 186.

[17] G. Zhu, Y. Su, P. Bai, J. Chen, Q. Jing, W. Yang, Z. L. Wang, *ACS Nano* **2014**, *8*, 6031.

[18] J. Chen, J. Yang, Z. Li, X. Fan, Y. Zi, Q. Jing, H. Guo, Z. Wen, K. C. Pradel, S. Niu, *ACS Nano* **2015**, *9*, 3324.

[19] J. Yin, Z. Zhang, X. Li, J. Yu, J. Zhou, Y. Chen, W. Guo, *Nat. Commun.* **2014**, *5*, 3582.

[20] J. Yin, X. Li, J. Yu, Z. Zhang, J. Zhou, W. Guo, *Nat. Nanotech.* **2014**, *9*, 378.

[21] Ü. Özgür, Y. I. Alivov, C. Liu, A. Teke, M. A. Reshchikov, S. Doğan, V. Avrutin, S.-J. Cho, H. Morkoç, *J. Appl. Phys.* **2005**, *98*, 041301.

[22] G. Zhu, R. Yang, S. Wang, Z. L. Wang, *Nano Lett.* **2010**, *10*, 3151.

[23] G. Redmond, D. Fitzmaurice, M. Graetzel, *Chem. Mater.* **1994**, *6*, 686.

[24] M. Izaki, T. Omi, *Appl. Phys. Lett.* **1996**, *68*, 2439.

[25] V. Vaithianathan, B.-T. Lee, S. S. Kim, *Appl. Phys. Lett.* **2005**, *86*, 2101.

[26] X. Xu, S. Lau, J. Chen, G. Chen, B. Tay, *J. Cryst. Growth* **2001**, *223*, 201.

[27] Y. Wang, S. Lau, H. Lee, S. Yu, B. Tay, X. Zhang, K. Tse, H. Hng, *J. Appl. Phys.* **2003**, *94*, 1597.

[28] S. Lee, H. Kim, D.-J. Yun, S.-W. Rhee, K. Yong, *Appl. Phys. Lett.* **2009**, *95*, 262113.

[29] P. F. Carcia, R. S. McLean, M. H. Reilly, G. Nunes, *Appl. Phys. Lett.* **2003**, *82*, 1117.

[30] J. Yin, Z. Zhang, X. Li, J. Zhou, W. Guo, *Nano Lett.* **2012**, *12*, 1736.

[31] G. Li, T. Chen, B. Yan, Y. Ma, Z. Zhang, T. Yu, Z. Shen, H. Chen, T. Wu, *Appl. Phys. Lett.* **2008**, *92*, 173104.

[32] X. Feng, L. Feng, M. Jin, J. Zhai, L. Jiang, D. Zhu, *J. Am. Chem. Soc.* **2004**, *126*, 62.

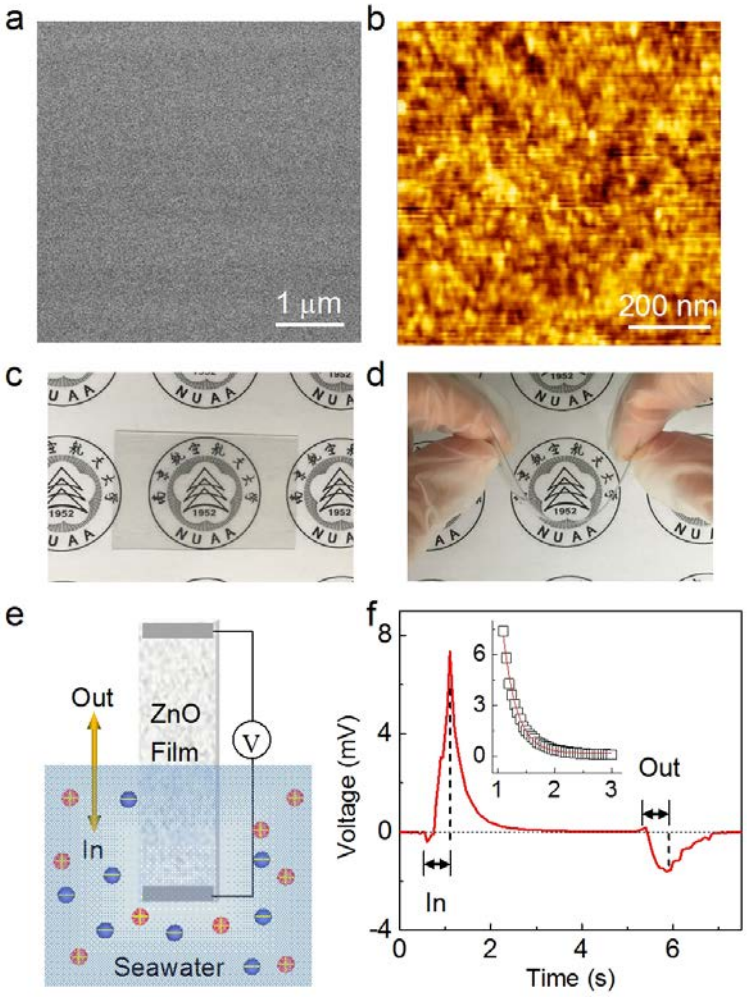

Fig.1 Generating electricity by moving transparent flexible ZnO nanofilm across the surface of simulated seawater (0.6 M NaCl). a,b) SEM (a) and AFM (b) images of the ZnO nanofilm. c,d) Photographs of the transparent and flexible ZnO nanofilm on PET. e) Schematic illustration of the experimental setup. f) Typical voltage signal produced across a sample moving into and out from the seawater at a velocity of 13.5 cm/s. The insert shows the exponential fit to the voltage drop section after completely immersing the sample into the solution.

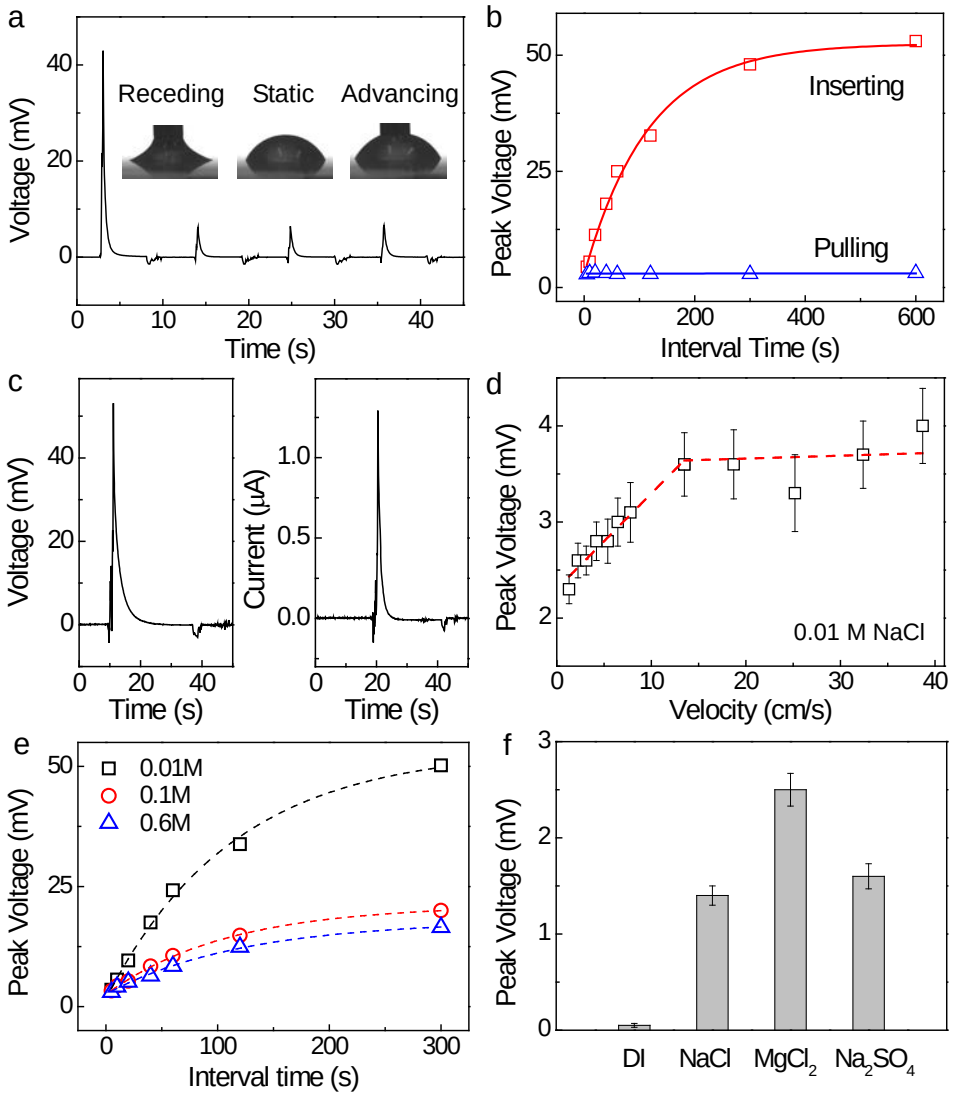

Fig. 2 Dependence of the voltage on various factors. a) Voltage signal induced during the first and following three cycles when moving the sample across the surface of 0.6 M NaCl solutions at a velocity of 18.7 cm/s. The inserts show the typical contact angles of the ZnO film. b) Peak voltage as a function of interval time between two cycles at 4.2 cm/s in 0.6 M NaCl solutions. The red and blue solid lines are exponential and linear fits to the inserting and pulling induced peak voltage respectively. c) Open-circuit voltage and short-circuit current when inserting ZnO nanofilm into 0.6 M NaCl solutions at 4.2 cm/s with a interval time of 10 min. d) Peak voltage as a function of velocity. The red solid lines are linear fits to the data at low ($v \leqslant 13.5$ cm/s) and high ($v \geqslant 13.5$ cm/s) velocity regions. e) Peak voltage as

a function of the interval time when inserting ZnO nanofilm into 0.01 M, 0.1 M, 0.6 M NaCl solutions, respectively, at 7.8 cm/s. The solid lines are exponential fittings. f) Peak voltage induced by inserting the ZnO nanofilm into DI water and NaCl, $MgCl_2$, Na_2SO_4 solution of the same 0.1 M concentration at 7.8 cm/s. The interval time between the measurements is 5 s.

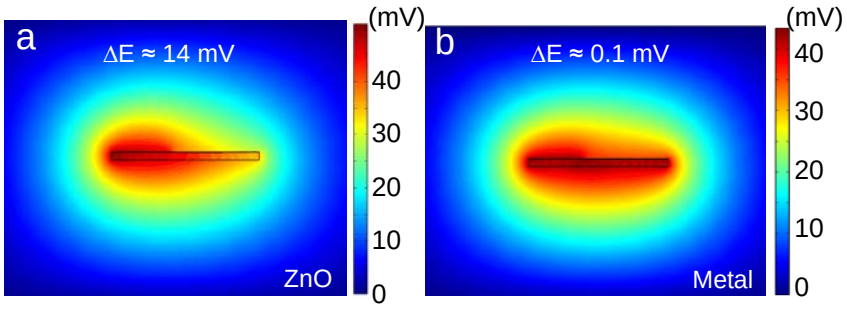

Fig. 3 Representative potential-distribution of the ZnO (a) and metal (b) nanofilm during the adsorption of cations on the left section simulated by the COMSOL multi-physics software.

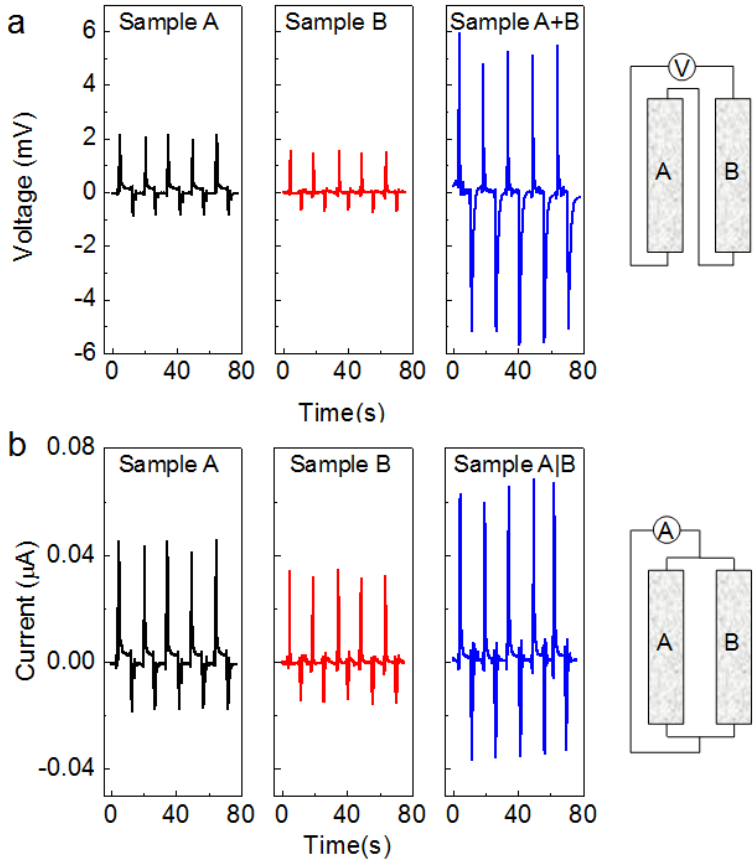

Fig. 4 Scalability of the harvesting electricity. a) Series connection of samples A and B moving across the surface of 0.1 M NaCl solution at v = 7.8 cm/s can amplify the open-circuit voltage (A+B). b) Parallel connection of the two samples can scale up the short-circuit current (A|B). The right panel shows the schematic images of the series and parallel connection.